Aalto University

Aaltodoc

OPEN ACCESS

Author(s): Äyräs, Pekka & Friberg, Ari T. & Kaivola, Matti & Salomaa, Martti M.

Title: Conoscopic interferometry of wafers for surface-acoustic wave devices

Year: 1997

Version: Final published version

Please cite the original version:

Conoscopic interferometry of wafers for surface-acoustic wave devices

P. Äyräs, A. T. Friberg, M. Kaivola, and M. M. Salomaa

Conoscopic interferometry of wafers for surface-acoustic wave devices

P. Äyräs
Department of Engineering Physics and Mathematics, Materials Physics Laboratory,
Helsinki University of Technology, FIN-02150 Espoo, Finland

A. T. Friberg[a]
Optisches Institut, Technische Universität Berlin, D-10623 Berlin, Germany

M. Kaivola and M. M. Salomaa[b]
Department of Engineering Physics and Mathematics, Materials Physics Laboratory,
Helsinki University of Technology, FIN-02150 Espoo, Finland

We show that in interpreting the conoscopic interference fringes, one should exercise care in employing approximate expressions which fail for certain crystal cuts. In this paper, we study 64°- and 128°-rotated Y-cut and Z-cut LiNbO$_3$ wafers. We show that the error made in using the approximate formulae for the samples is more than 25% and that one has to use exact formulae in order to attain quantitative agreement with the experimental data. © *1997 American Institute of Physics.* [S0021-8979(97)04619-7]

INTRODUCTION

Recently, Jen and Hartmann[1] described how the orientation of uniaxial crystals applied as substrates for surface-acoustic wave (SAW) devices may conveniently be determined optically. The orientation was established with conoscopic interference for several crystals and crystal cuts commonly used in SAW components. The authors concluded that the method is best suited for a relative comparison among wafers from a discrete set. We propose to use conoscopic interference as a quantitative tool for determining the orientation of SAW wafers. However, we find that the approximate formulae used by Jen and Hartmann do not yield accurate results. Therefore, in this paper we employ more precise expressions for crystal optics which we demonstrate to provide improved fits to experimental data. In particular, we study 64°- and 128°-rotated Y-cut and Z-cut LiNbO$_3$ wafers.

Conoscopic interferometry is a well-established method for studying the optical properties of birefringent crystals. The basic structure of a conoscope is simple,[2,3] which makes it convenient for laboratory use as a quick identification method. Conoscopic interference is based on the fact that light propagating in birefringent crystals is divided into two mutually orthogonal polarization components (the electric displacement vectors for the two rays are perpendicular to each other). The two components traverse the sample with unequal velocities and the light becomes elliptically polarized. By analyzing the polarization state of the outcoming light with a linear polarizer, interference fringes become visible. The shape, intensity and density of the fringes depend on the optical properties of the sample. Owing to the birefringence of several minerals, conoscopic interference is widely used in mineralogy for sample identification.[4] In fabricating SAW components it is vital to know the crystal orientation precisely since the propagation of SAWs strongly depends on the wave-propagation direction.[5]

EXPERIMENTAL TECHNIQUE

In this paper we use a conoscope setup similar to the one of Ohtsuka *et al.*,[2] (see Fig. 1). The birefringent sample is illuminated with a converging beam of linearly polarized light. As the source of light, we use a 1.7 mW He–Ne laser ($\lambda = 632.8$ nm). The spot size on the sample is about 1 mm. As light emerges from the sample, it is analyzed with a crossed polarizer. Interferograms are recorded on the screen 28 mm from the sample. The shape and the density of the fringes depend on the material and thickness of the sample and on the direction of the optic axes. For uniaxial crystals, the interference fringes are families of conic sections.

ANALYSIS

The phase difference between the two rays may be evaluated as reported in the literature.[6] Upon traversing a crystal slab of thickness h, the two rays acquire an optical phase difference of

$$\delta = \frac{2\pi h}{\lambda}(n'' \cos \theta'' - n' \cos \theta'),\tag{1}$$
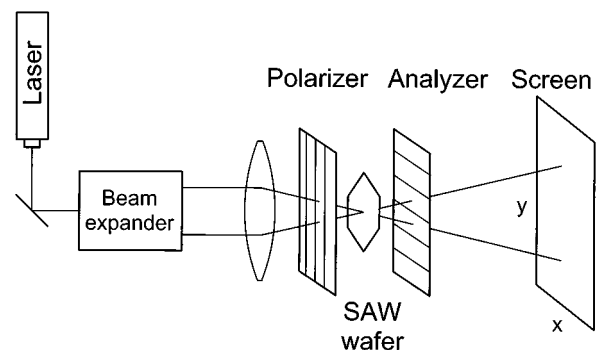

FIG. 1. Structure of a conoscope. The shape and density of the interference fringes on the screen depend on the direction of the optic axes and on the optical properties of the sample.

[a]Permanent address: Dept. of Physics, University of Joensuu, P.O. Box 111, FIN-80101 Joensuu, Finland.
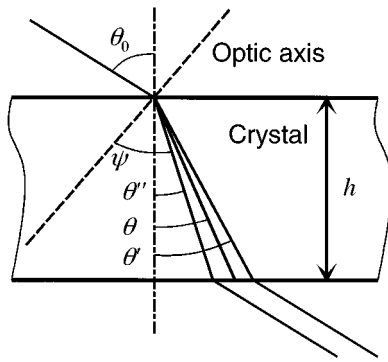[b]Electronic mail:Martti.Salomaa@hut.fi

FIG. 2. Definitions of the angles used in the calculations for uniaxial crystals. The angles of refraction for the two rays are θ' and θ''; their average is θ. The angle between the extraordinary ray and the optic axis is denoted as ψ.

where λ is the wavelength of light in vacuum and θ', θ'' and n', n'', respectively, are the angles and indices of refraction for the two rays in the crystal. The geometry of the refracted rays is indicated in Fig. 2. Equation (1) is valid for both uniaxial and biaxial crystals. In general, both n' and n'' depend on the direction of ray propagation. However, for uniaxial crystals only the refractive index for the extraordinary ray, n'', depends on the direction of ray propagation while the one for the ordinary ray, n', is a constant. The values for the two refractive indices are

$$n'^2 = n_o^2; \quad n''^2 = n_o^2 + (n_e^2 - n_o^2)\sin^2 \psi, \tag{2}$$

where ψ is the angle between the extraordinary ray and the optic axis and n_o and n_e are the refractive indices for the ordinary and extraordinary rays along the principal dielectric axes. We emphasize that Eq. (1) is exact within ray optics. The indices n' and n'' may be related to the angles θ' and θ'' by applying Snell's law, which yields $n' \sin \theta' = n'' \sin \theta''$, where one must take into account the angular dependence of n''. In this connection, simplifying approximations are often made, as specified below. Observe that because of the refraction at the exit surface, Eq. (1) is implicit and we determine the phase difference on the screen iteratively.
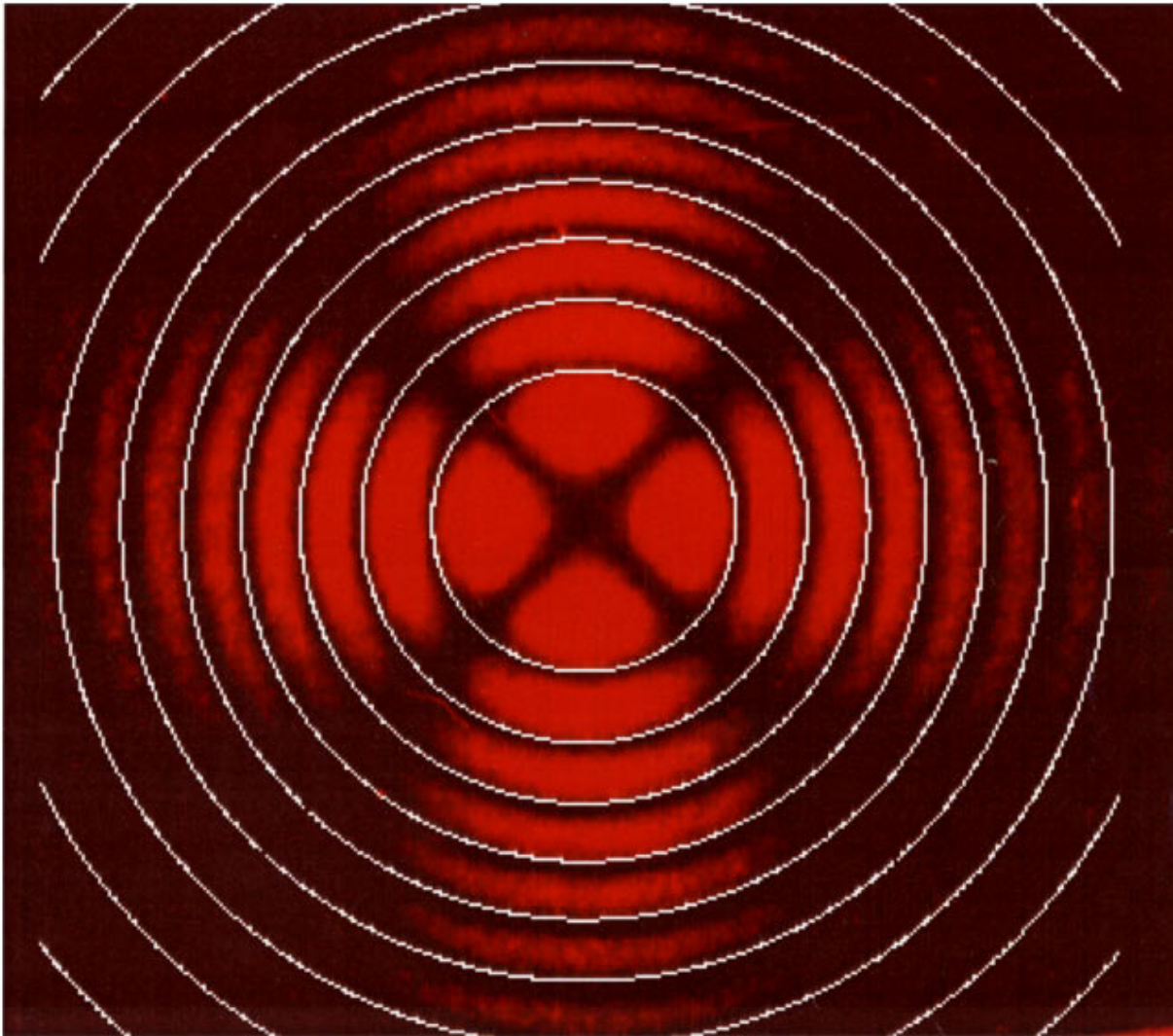

FIG. 3. Interferogram for a Z-cut LiNbO$_3$ wafer with the calculated curves superimposed on the measured data. Here the optic axis is perpendicular to the plane of the paper. The two ''dark brushes'' (crossed zeroes in intensity) are in the directions of the polarizer and analyzer.
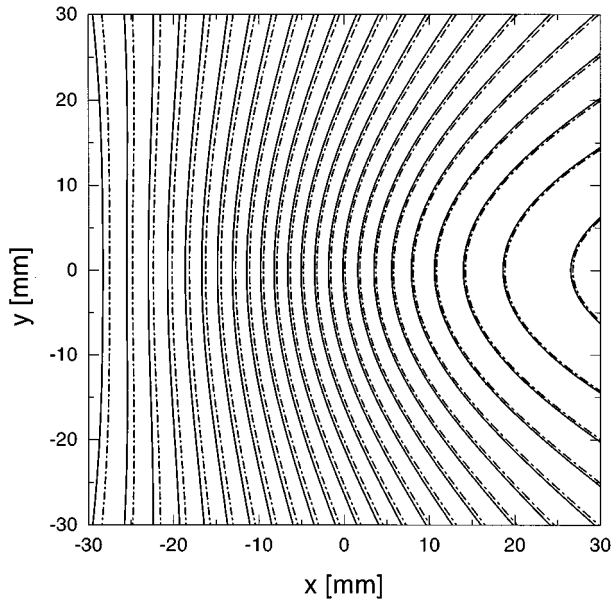
FIG. 4. Calculated fringes for a 64°-rotated Y-cut LiNbO$_3$ wafer. Solid curves are calculated with the exact formula, Eq. (1), dashed-dotted with the approximate one, Eq. (4). The difference between the two curves increases with the angle ψ.
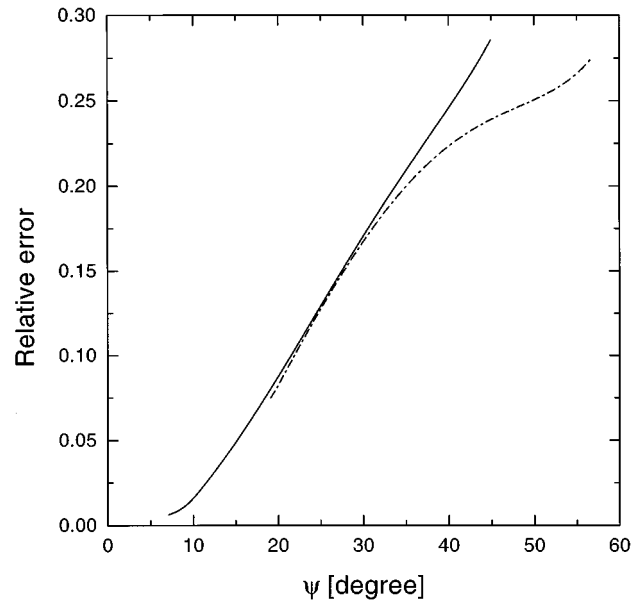
FIG. 5. Relative error of the approximate interferogram in Fig. 4, calculated for $y=0$ (solid). The error is the difference between the exact and the approximate locus divided by the distance between two successive fringes. For comparison, the equivalent curve for 128° is also shown (dashed-dotted).

FIG. 6. Interference fringes for a 64°-rotated Y-cut LiNbO$_3$ wafer and the calculated interferogram. The ''dark brushes'' due to Malus' law (cf. Fig. 3) are here situated outside the image area.

It is customary to approximate Eq. (1) by assuming that the ordinary and extraordinary rays propagate equal distances in the crystal. Thus, in this approximation, the phase difference on the back surface of the sample is

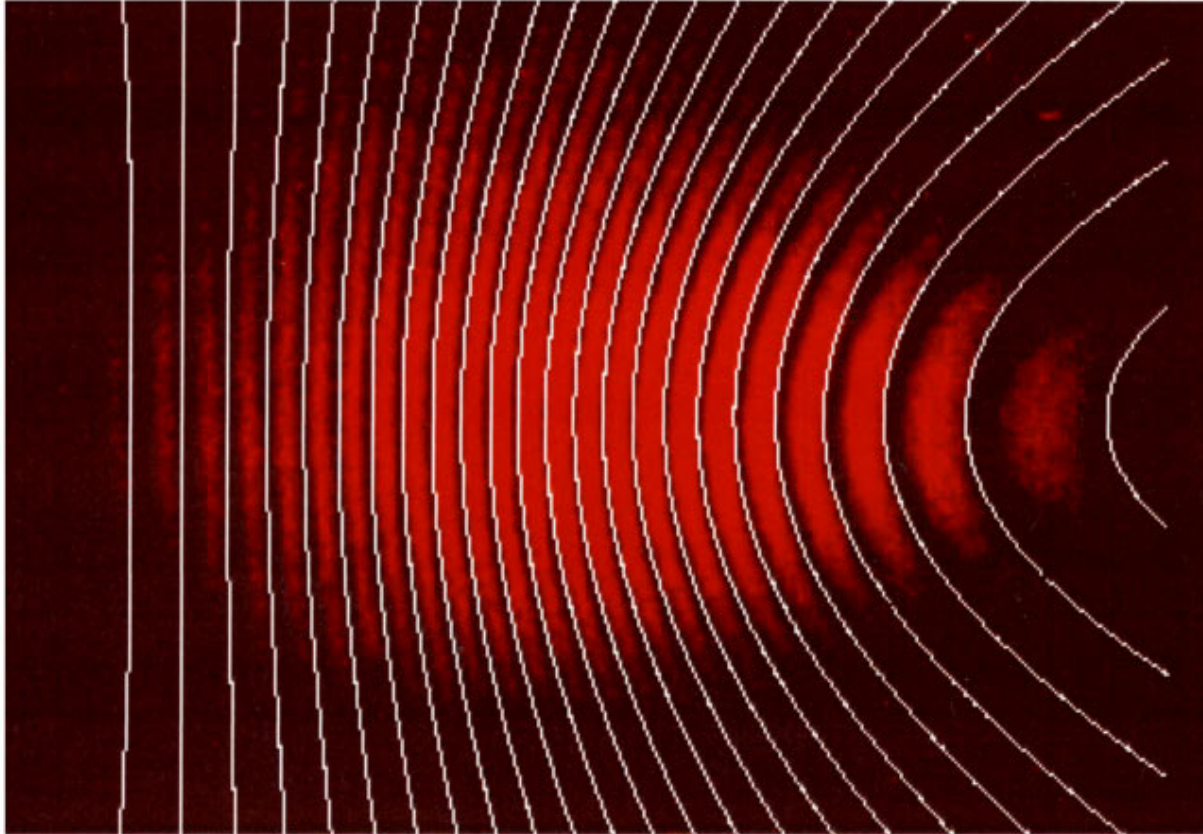$$\delta = \frac{2\pi h}{\lambda \cos \theta}(n'' - n'), \qquad (3)$$

where $\theta = (\theta' + \theta'')/2$ and $h/\cos \theta$ is the average geometrical path of the two rays (see Fig. 2). When $n'' - n' \ll n'$, n'' one finds with the aid of Eq. (2) a simple approximate form for the phase difference[6]

$$\delta = \frac{2\pi h}{\lambda \cos \theta}(n_e - n_o)\sin^2 \psi. \qquad (4)$$

This equation is only valid for uniaxial crystals. The deceiving simplicity in the application of this equation is due to the feature that one need not calculate the angular dependence of the refractive indices.

RESULTS

The measured and calculated interferogram for a Z-cut LiNbO$_3$ wafer is superposed in Fig. 3 where the interference pattern is calculated using Eq. (1). Here the optic axis is perpendicular to the plane of the paper and the interference fringes form concentric circles. The dark lines in the figure are in the directions of the polarization axes of the polarizer and analyzer. The pattern arises as the result of pure mode propagation, i.e., with either the ordinary or extraordinary ray propagating in these directions. The pure modes are extinguished in the crossed polarizer. Similar ''dark brushes'' appear for other orientations as well, in accordance with Malus' law. However, by choosing the directions of the polarizer and analyzer suitably, the brushes for them are projected outside the detected area of the interferogram. The orientation of the optic axis of the sample is determined by comparing the calculated interferogram with the measured one. Values for the sample thickness were provided by the manufacturer; values for indices of refraction are derived from the literature.[7]

DISCUSSION

We compare our experiments with the interferograms calculated with both the exact and the approximate formulae. The difference between the fringe patterns calculated with these two formulae is visualized in Fig. 4: the two families of graphs differ substantially. These differences are relevant as one tries to quantitatively fit the calculated interferogram with the measured one. Figure 5 shows how the relative error in the approximate expression increases with ψ. The data are for the same 64°-rotated wafer as in Fig. 4 and calculated at $y = 0$. Similar investigations are made for the 128° wafer; the shape of the curve is different but the relative error is of the same order.

The samples we use are commercial SAW wafers. One side of the sample is polished while the other is rough. The exit surface of the sample must be polished, otherwise the scattering of light destroys the interference pattern. The entrance surface may well be unpolished and this feature can, in fact, be used to an advantage.[1] The scattering of light at the front surface increases the radiation cone within the crystal, and thus one sees a larger interferogram on the screen.

In Fig. 6, the interferogram calculated using Eq. (1) is superposed onto a recorded interferogram for a 64°-rotated Y-cut LiNbO$_3$ wafer. It is seen that now the fitting is fair. The interferograms are evaluated for destructive interference since this makes the fitting more precise, due to the property that the dark lines are thinner than the bright ones in the recorded data. The most crucial part in the fitting is the area where the fringes are densest. All the wafers studied are optically uniaxial (like the wafers commonly used in SAW devices). Biaxial crystals may also be studied with conoscopic interference; for lack of space these results will be presented elsewhere.

In conclusion, like Jen and Hartmann, we find that conoscopic interference is convenient for quickly identifying samples from a discrete set; it is used for determining the orientation of SAW wafers in industrial applications. We have shown that the approximate expression for the phase difference is inadequate for quantitative analysis; we propose to improve conoscopic interferometry to provide an accurate method for determining the orientation of SAW wafers.

ACKNOWLEDGMENTS

[1] S. Jen and C. S. Hartmann, IEEE Ultrasonic Symposium Proceedings, 1994, pp. 397–401.
[2] K. Ohtsuka, H. Ara, and T. Ogawa, Jpn. J. Appl. Phys., Part 1 **23**, 1541 (1984).
[3] X. Zhou and X. Xu, Cryst. Res. Technol. **31**, K9 (1996).
[4] N. H. Hartshorne and A. Stuart, *Practical Optical Crystallography* (Edward Arnold, London, 1969).
[5] D. P. Morgan, *Surface-Wave Devices for Signal Processing* (Elsevier, Amsterdam, 1991).
[6] M. Born and E. Wolf, *Principles of Optics* (Pergamon, Oxford, 1980).
[7] *Handbook of Chemistry and Physics*, edited by R. C. Weast (CRC, Bora Raton, FL, 1986).